# Exploring d–d and d–f Coupled Ba-Based Double Perovskites for Spintronic and Thermoelectric Applications: A First-Principles Study

**Lalmuanawma Chhangte[1], Lalnunpuia[2,*], Lalrintluanga Sailo[3], Lawrence Zonunmawia[3], Remlalsiama[3], Zaithanzauva Pachuau[4], Malsawmtluanga[5], T Malsawmtluanga[1]**

[1]Department of Physics, Lunglei Govt. College, Lunglei, Mizoram, India

[2]Department of Physics, Govt. Champhai College, Champhai, Mizoram, India

[3]Department of Physics, Govt. Zirtiri Res. Sc. College, Aizawl, Mizoram, India

[4]Department of Physics, Mizoram University, Aizawl, Mizoram, India

[5]Research Scholar, Mizoram University, Aizawl, Mizoram, India

[*]Corresponding Author: lnpuia@gmail.com

**Abstract**

In this work, we present a first-principles investigation of the structural, electronic, magnetic, elastic, and thermoelectric properties of Ba-based double perovskites $Ba_2MnTaO_6$ and $Ba_2TmTaO_6$ using density functional theory. Both compounds are found to be structurally stable in the cubic phase. $Ba_2MnTaO_6$ exhibits half-metallic ferromagnetism with a high magnetic moment, indicating its suitability for spintronic applications. In contrast, $Ba_2TmTaO_6$ shows half-metallic behavior with nearly complete spin polarization, governed by the presence of localized f-electron states. Electronic structure analysis reveals strong hybridization between Mn-d and O-p states, while Tm-f states dominate near the Fermi level in $Ba_2TmTaO_6$. The calculated elastic constants confirm mechanical stability with anisotropic and brittle characteristics. Thermoelectric properties, evaluated using Boltzmann transport theory, demonstrate an increase in electrical conductivity and Seebeck coefficient with temperature, resulting in an enhanced power factor. These findings highlight the role of d–d and d–f interactions in tuning multifunctional properties, making $Ba_2MnTaO_6$ and $Ba_2TmTaO_6$ promising candidates for spintronic and thermoelectric applications.

**Keywords:** Double perovskites; Density functional theory (DFT); Half-metallicity; Spintronics; Thermoelectric properties.

## 1. Introduction

Perovskite and double perovskite oxides have attracted significant attention due to their rich structural flexibility and diverse multifunctional properties. The general formula $A_2BB'O_6$ allows the incorporation of different transition and rare-earth elements at the B and B′ sites, leading to a wide range of electronic, magnetic, and transport behaviors [1]. Early studies on perovskite oxides highlighted their potential in applications such as superconductivity, magnetoresistance, and ferroelectricity, establishing them as an important class of functional materials [2].

In recent years, Ba-based double perovskites have emerged as promising candidates for advanced technological applications due to their structural stability and tunable properties. The presence of alkaline-earth metal Ba at the A-site enhances lattice stability, while the combination of transition metal and rare-earth ions at the B-sites enables control over electronic correlations and magnetic ordering [3]. In particular, transition metal-based systems such as $Ba_2MnTaO_6$ have been reported to exhibit half-metallic ferromagnetism, a key requirement for spintronic devices where 100% spin polarization is desirable [4].

Simultaneously, rare-earth-based double perovskites, such as $Ba_2TmTaO_6$, have gained attention due to the involvement of localized f-electrons, which introduce strong electron correlation effects and significantly influence the electronic structure [5]. The interplay between d–d and d–f interactions in such systems provides a pathway to engineer novel electronic phases and enhance functional performance. Moreover, the growing demand for efficient energy conversion technologies has stimulated interest in the thermoelectric properties of these materials, where a

high Seebeck coefficient combined with good electrical conductivity is essential [6].

Despite these advancements, a systematic comparative understanding of Ba-based double perovskites involving both transition metal and rare-earth elements remains limited. In this context, the present study focuses on a detailed first-principles investigation of $Ba_2MnTaO_6$ and $Ba_2TmTaO_6$ to explore their structural, electronic, magnetic, elastic, and thermoelectric properties. The aim is to elucidate the role of d–d and d–f electronic interactions in determining their multifunctional behavior and to assess their suitability for spintronic and thermoelectric applications.

## 2. Computational Methodology

The structural, electronic, magnetic, elastic and thermoelectric properties of $Ba_2MnTaO_6$ and $Ba_2TmTaO_6$ were investigated using density functional theory (DFT) within the framework of the full-potential linearized augmented plane wave (FP-LAPW) method as implemented in the WIEN2k code [7]. The exchange–correlation potential was described using the generalized gradient approximation (GGA) in the Perdew–Burke–Ernzerhof (PBE) scheme [8]. To obtain an accurate description of the electronic structure, particularly for systems involving correlated d and f electrons, the modified Becke–Johnson (mBJ) potential was employed [9].

The muffin-tin radii ($R_{MT}$) were selected carefully to avoid overlap between atomic spheres and the plane-wave cutoff parameter was set to $R_{MT} \times K_{max} = 7$, ensuring good convergence of the basis set. The Brillouin zone integrations were performed using a dense Monkhorst–Pack k-point mesh consisting of approximately 3000 k-points in the irreducible wedge. Self-consistency was achieved with convergence criteria of $10^{-4}$ Ry for total energy and $10^{-4}$ *e* for charge density.

Structural optimization was carried out using the Birch–Murnaghan equation of state [4] to determine equilibrium lattice parameters, ground-state energy and bulk modulus. Spin-polarized calculations were performed to identify the magnetic ground state of the compounds. The elastic constants were calculated using the energy-strain method, where small distortions were applied to the optimized structure to extract second-order elastic constants and evaluate mechanical stability.

Thermoelectric properties were computed using the semi-classical Boltzmann transport theory within the constant relaxation time approximation, as implemented in the BoltzTraP code [10]. A dense k-point mesh of 150,000 points was used to accurately calculate transport coefficients such as electrical conductivity, Seebeck coefficient, and power factor as functions of temperature.

## 3. Results and Discussion

### 3.1 Structural Properties

The structural properties of $Ba_2MnTaO_6$ and $Ba_2TmTaO_6$ were investigated by optimizing the total energy as a function of unit cell volume using the Birch–Murnaghan equation of state [4]. The corresponding energy–volume curves are presented in Fig. 1, where a clear minimum in total energy confirms the thermodynamic stability of both compounds in their ground state. The smooth parabolic behavior of the curves indicates reliable convergence and accuracy of the calculations.

Both compounds are found to crystallize in the cubic double perovskite structure with space group $Fm\bar{3}m$, consistent with previous reports on Ba-based systems [11]. The optimized lattice parameters are summarized in Table 1. The lattice constant of $Ba_2MnTaO_6$ is calculated to be 8.10 Å, while $Ba_2TmTaO_6$ shows a slightly larger value of 8.44 Å. This increase can be attributed to the larger ionic radius and localized nature of Tm-f electrons compared to Mn-d electrons [13].

The bulk modulus values further provide insight into the mechanical rigidity of the compounds. $Ba_2MnTaO_6$ exhibits a higher bulk modulus (170.67 GPa) than $Ba_2TmTaO_6$ (149.34 GPa), indicating stronger interatomic bonding in the Mn-based system. This behavior is primarily associated with stronger d–p hybridization in transition metal oxides.

Structurally, both compounds consist of corner-sharing $TaO_6$ and $MnO_6$/$TmO_6$ octahedra, with Ba atoms occupying the A-site and coordinated by twelve oxygen atoms. The equality of Ta–O and M–O bond lengths confirm the high symmetry of the cubic phase. Additionally, the negative total energy values listed in Table 1 further verify the energetic stability of the studied compounds.

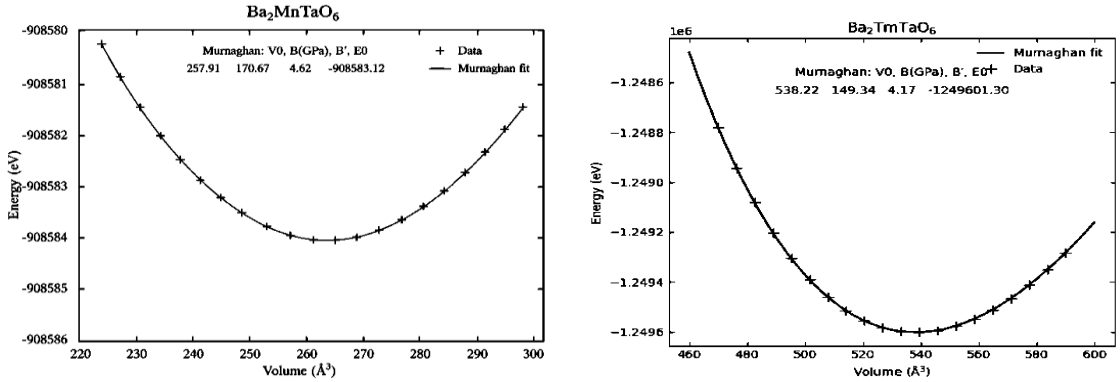


(a) (b)

**Fig. 1. Energy–volume (E–V) curve of (a) $Ba_2MnTaO_6$ in the ferromagnetic (FM) phase and (b) $Ba_2TmTaO_6$ in the paramagnetic (PM) phase, fitted using the Murnaghan equation of state.**

**Table 1. Optimized structural parameters of $Ba_2MnTaO_6$ and $Ba_2TmTaO_6$.**

| Parameters | $Ba_2MnTaO_6$ | $Ba_2TmTaO_6$ |
|---|---|---|
| a (Å) Present | 8.10 | 8.44 |
| Theory | 8.13 [12] | 8.40–8.41 [11,13] |
| B (GPa) | 170.67 | 149.34 |
| B′ | 4.62 | 4.17 |
| V (Å³) | 257.91 | 538.22 |
| E (eV) | −908583.12 | −1249601.3 |

Overall, the analysis of Fig. 1 and Table 1 confirms that $Ba_2MnTaO_6$ and $Ba_2TmTaO_6$ are structurally stable cubic double perovskites, providing a solid basis for further investigation of their electronic and transport properties.

### 3.2 Electronic and Magnetic Properties

The electronic structure of $Ba_2MnTaO_6$ and $Ba_2TmTaO_6$ was investigated using spin-polarized calculations within the mBJ potential [9]. The calculated band structures along high-symmetry directions are shown in Fig. 2, while the corresponding total density of states (DOS) is presented in Fig. 3.

For $Ba_2MnTaO_6$, the band structure (Fig. 2(a)) clearly exhibits half-metallic behavior, with a metallic spin-up channel and a semiconducting spin-down channel having a direct band gap of approximately 2.24 eV at the Γ-point. This results in complete spin polarization at the Fermi level, which is highly desirable for spintronic applications. The total DOS confirms that the states near the Fermi level are primarily dominated by Mn-*d* states with hybridization from O-*p* orbitals.

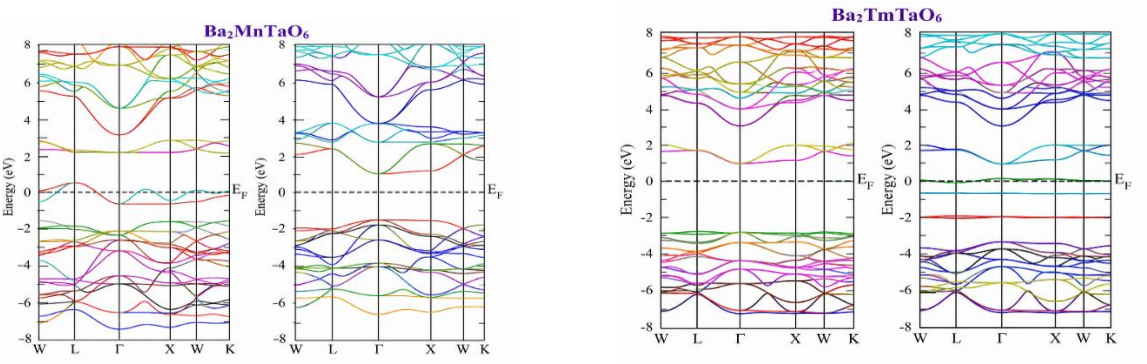


(a) (b)

**Fig. 2. Band structure of (a) $Ba_2MnTaO_6$ and, (b) $Ba_2TmTaO_6$**

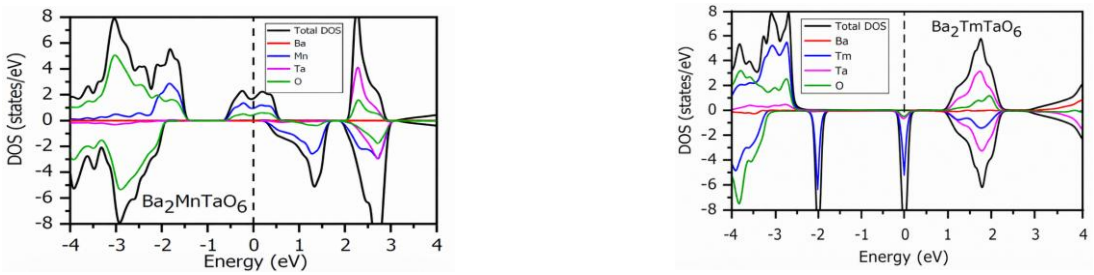


(a) (b)

**Fig. 3. Density of states (DOS) in (a) $Ba_2MnTaO_6$ and, (b) $Ba_2TmTaO_6$**

In the case of $Ba_2TmTaO_6$, the band structure (Fig. 2(b)) also indicates half-metallicity, where one spin channel is metallic while the other shows semiconducting behavior. The electronic states near the Fermi level are mainly influenced by localized Tm-*f* states, which play a crucial role in determining the spin-dependent electronic properties.

From a magnetic perspective, $Ba_2MnTaO_6$ stabilizes in a ferromagnetic ground state with a total magnetic moment of approximately 4 μB, arising mainly from Mn ions. In contrast, $Ba_2TmTaO_6$ exhibits a paramagnetic ground state due to the localized nature of *f*-electrons.

Overall, both compounds exhibit half-metallic characteristics; however, the origin of this behavior differs significantly, with $Ba_2MnTaO_6$ governed by *d*-electron interactions and $Ba_2TmTaO_6$ dominated by *f*-electron contributions.

### 3.3 Elastic Properties

The elastic properties of $Ba_2MnTaO_6$ and $Ba_2TmTaO_6$ were investigated to evaluate their mechanical stability and resistance to deformation. The calculated second-order elastic constants and derived mechanical parameters are summarized in Table 2.

**Table 2. Elastic constants and mechanical parameters of $Ba_2MnTaO_6$ and $Ba_2TmTaO_6$.**

| Parameter | $Ba_2MnTaO_6$ | $Ba_2TmTaO_6$ |
|---|---|---|
| $C_{11}$ (GPa) | 157.3 | 263.3 |
| $C_{12}$ (GPa) | 69.4 | 32.3 |
| $C_{44}$ (GPa) | 74.1 | 60.4 |
| B (GPa) | 98.7 | 109.3 |
| G (GPa) | 95.3 | 85.0 |
| Y (GPa) | 216.2 | 202.5 |
| B/G | 1.03 | 1.28 |
| ν | 0.13 | 0.19 |

For cubic crystals, the mechanical stability criteria require $C_{11} > 0$, $C_{44} > 0$, $C_{11} - C_{12} > 0$, and $C_{11} + 2C_{12} > 0$ [14]. The calculated elastic constants satisfy all these conditions, confirming that both compounds are mechanically stable.

The bulk modulus (B) and shear modulus (G) were obtained using the Voigt–Reuss–Hill approximation [15], and the corresponding Young's modulus (Y) reflects the stiffness of the materials. $Ba_2TmTaO_6$ exhibits a higher bulk modulus, indicating stronger resistance to volume compression, whereas $Ba_2MnTaO_6$ shows slightly higher shear resistance.

The ductility or brittleness of the materials was evaluated using Pugh's ratio (B/G) [16]. Since the B/G values for both compounds are less than 1.75, they are classified as brittle. This is further supported by the low Poisson's ratio values ($\nu \approx 0.13$–$0.19$), which fall within the typical brittle range [17]. Additionally, the negative Cauchy pressure values confirm the brittle nature of these materials.

Overall, the elastic analysis demonstrates that $Ba_2MnTaO_6$ and $Ba_2TmTaO_6$ are mechanically stable, stiff, and brittle materials with anisotropic characteristics, consistent with previous theoretical studies on oxide perovskites [18].

### 3.4 Thermoelectric Properties

The thermoelectric properties of $Ba_2MnTaO_6$ and $Ba_2TmTaO_6$ were investigated using Boltzmann transport theory within the constant relaxation time approximation [10]. The temperature dependence of electrical conductivity ($\sigma/\tau$), electronic thermal conductivity ($\kappa/\tau$), and Seebeck coefficient (S) is presented in Figs. 4–6 .

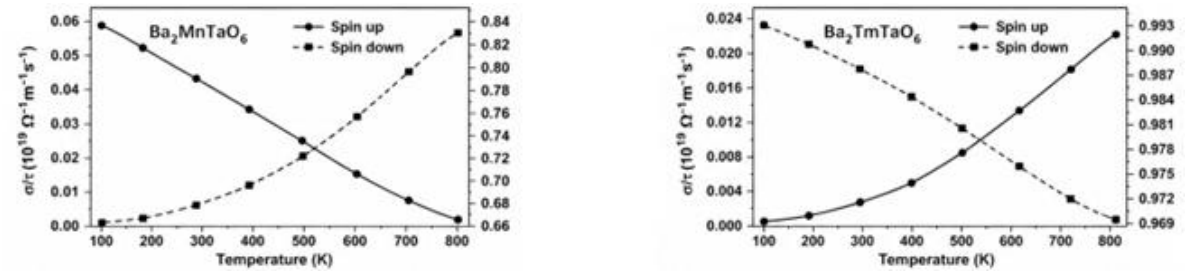


(a) (b)

**Fig. 4. Electrical conductivity ($\sigma/\tau$) as a function of temperature for (a) $Ba_2MnTaO_6$ and (b) $Ba_2TmTaO_6$.**

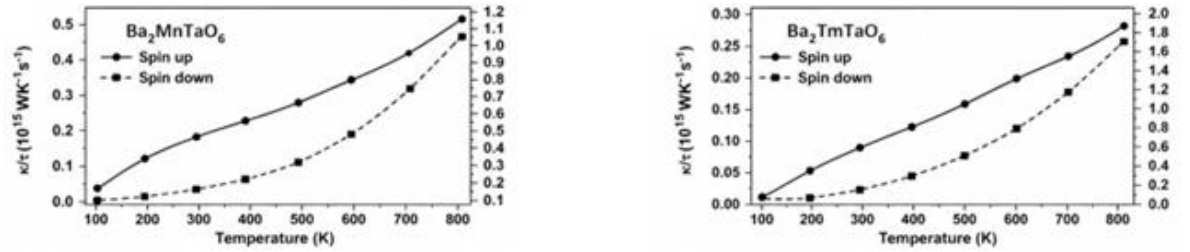


(a) (b)

**Fig. 5. Electronic thermal conductivity ($\kappa/\tau$) as a function of temperature for (a) $Ba_2MnTaO_6$ and (b) $Ba_2TmTaO_6$.**


(a) (b)

**Fig. 6. Seebeck coefficient (S) as a function of temperature for (a) $Ba_2MnTaO_6$ and (b) $Ba_2TmTaO_6$.**

The electrical conductivity ($\sigma/\tau$), shown in Fig. 4(a–b), exhibits strong spin-dependent behavior for both compounds. In $Ba_2MnTaO_6$ (Fig. 4a), the spin-up channel decreases monotonically with temperature, indicating metallic behavior due to enhanced electron scattering, whereas the spin-down channel increases with temperature, reflecting semiconducting characteristics. Conversely, $Ba_2TmTaO_6$ (Fig. 4b) shows an opposite trend, where the spin-up channel increases with temperature while the spin-down channel decreases, further confirming the half-metallic nature of both materials.

The variation of electronic thermal conductivity ($\kappa/\tau$) with temperature is illustrated in Fig. 5(a–b). For $Ba_2MnTaO_6$ (Fig. 5a), both spin channels show an increasing trend with temperature, with a more pronounced rise in the spin-down

channel at higher temperatures. Similarly, $Ba_2TmTaO_6$ (Fig. 5b) exhibits an almost linear increase in $\kappa/\tau$ for both spin channels, indicating enhanced carrier contribution to heat transport at elevated temperatures.

The Seebeck coefficient (S), depicted in Fig. 6(a–b), shows contrasting behavior between the two spin channels. In $Ba_2MnTaO_6$ (Fig. 6a), the spin-up component increases with temperature, while the spin-down component decreases sharply. In contrast, $Ba_2TmTaO_6$ (Fig. 6b) shows a decreasing trend in the spin-up channel and an increasing trend in the spin-down channel. This opposite variation between $\sigma/\tau$ and S is consistent with the inverse relationship between electrical conductivity and thermopower.

Overall, the thermoelectric performance of both compounds is strongly temperature dependent, with enhanced transport properties at higher temperatures. The interplay between metallic and semiconducting spin channels, governed by d-electron (Mn) and f-electron (Tm) contributions, plays a crucial role in determining their thermoelectric behavior, making these materials promising candidates for spin-dependent thermoelectric applications.

## 6. Conclusion

In this work, a comprehensive first-principles investigation of the structural, electronic, magnetic, elastic, and thermoelectric properties of $Ba_2MnTaO_6$ and $Ba_2TmTaO_6$ double perovskites has been carried out using the FP-LAPW method within the framework of density functional theory. The structural analysis confirms that both compounds are stable in the cubic phase, with optimized lattice parameters in good agreement with reported data.

The electronic structure reveals that both materials exhibit half-metallic behavior, characterized by metallic nature in one spin channel and semiconducting behavior in the other. $Ba_2MnTaO_6$ shows robust ferromagnetism with a magnetic moment of approximately 4 μB, while $Ba_2TmTaO_6$ exhibits paramagnetic characteristics dominated by localized f-electron states. These findings highlight the distinct roles of *d–d* and *d–f* interactions in determining their electronic and magnetic properties.

The calculated elastic constants satisfy the mechanical stability criteria, confirming that both compounds are mechanically stable and exhibit brittle behavior with anisotropic characteristics.

Thermoelectric analysis demonstrates strong temperature-dependent transport properties. The electrical conductivity, thermal conductivity, and Seebeck coefficient exhibit pronounced spin-dependent behavior, reflecting the half-metallic nature of the compounds. The interplay between metallic and semiconducting channels enhances the thermoelectric performance, particularly at higher temperatures. Overall, the combined properties of half-metallicity, magnetic ordering, mechanical stability, and favorable thermoelectric response suggest that $Ba_2MnTaO_6$ and $Ba_2TmTaO_6$ are promising candidates for multifunctional applications in spintronic and thermoelectric devices.

## References

[1] Kobayashi, K.-I., Kimura, T., Sawada, H., Terakura, K., & Tokura, Y. (1998). Room-temperature magnetoresistance in an oxide material with an ordered double-perovskite structure. *Nature, 395*, 677–680. https://doi.org/10.1038/27167

[2] Tokura, Y. (2006). Critical features of colossal magnetoresistive manganites. *Reports on Progress in Physics, 69*, 797. https://doi.org/10.1088/0034-4885/69/3/R06

[3] Vasala, S., & Karppinen, M. (2015). $A_2B'B''O_6$ perovskites: A review. *Progress in Solid State Chemistry, 43*, 1–36. https://doi.org/10.1016/j.progsolidstchem.2014.08.001

[4] Serrate, D., De Teresa, J. M., & Ibarra, M. R. (2007). Double perovskites with ferromagnetism above room temperature. *Journal of Physics: Condensed Matter, 19*, 023201. https://doi.org/10.1088/0953-8984/19/2/023201

[5] Coey, J. M. D. (2002). Half-metallic ferromagnets: Examples and applications. *Journal of Applied Physics, 91*, 8345. https://doi.org/10.1063/1.1451874

[6] Snyder, G. J., & Toberer, E. S. (2008). Complex thermoelectric materials. *Nature Materials, 7*, 105–114. https://doi.org/10.1038/nmat2090

[7] Blaha, P., Schwarz, K., Madsen, G. K. H., Kvasnicka, D., & Luitz, J. (2001). *WIEN2k: An augmented plane wave + local orbitals program for calculating crystal properties*.

[8] Perdew, J. P., Burke, K., & Ernzerhof, M. (1996). Generalized gradient approximation made simple. *Physical Review Letters, 77*, 3865. https://doi.org/10.1103/PhysRevLett.77.3865

[9] Tran, F., & Blaha, P. (2009). Accurate band gaps of semiconductors and insulators with a semilocal exchange-correlation potential. *Physical Review Letters, 102*, 226401. https://doi.org/10.1103/PhysRevLett.102.226401

[10] Madsen, G. K. H., & Singh, D. J. (2006). BoltzTraP: A code for calculating band-structure dependent quantities. *Computer Physics Communications, 175*, 67–71. https://doi.org/10.1016/j.cpc.2006.03.007

[11] Vasala, S., & Karppinen, M. (2015). $A_2B'B''O_6$ perovskites: A review. *Progress in Solid State Chemistry, 43*, 1–36. https://doi.org/10.1016/j.progsolidstchem.2014.08.001

[12] Gupta, D. C., & Nabi, M. (2015). First-principles study of $Ba_2MTaO_6$ (M = Cr, Mn). *Journal of Magnetism and Magnetic Materials, 377*, 234–240. https://doi.org/10.1016/j.jmmm.2014.10.081

[13] Azad, A. M., Subramanian, M. A., & others. (2009). Structural properties of double perovskites. *Journal of Solid State Chemistry, 182*, 289–295. https://doi.org/10.1016/j.jssc.2008.10.015

[14] Born, M., & Huang, K. (1954). *Dynamical theory of crystal lattices*. Oxford University Press. https://doi.org/10.1098/rspa.1954.0256

[15] Hill, R. (1952). The elastic behaviour of a crystalline aggregate. *Proceedings of the Physical Society A, 65*, 349. https://doi.org/10.1088/0370-1298/65/5/307

[16] Pugh, S. F. (1954). Relations between the elastic moduli and the plastic properties of polycrystalline pure metals. *Philosophical Magazine, 45*, 823. https://doi.org/10.1080/14786440808520496

[17] Nye, J. F. (1985). *Physical properties of crystals*. Oxford University Press. https://doi.org/10.1093/oso/9780198511656.001.0001

[18] Ravindran, P., Fast, L., Korzhavyi, P. A., Johansson, B., Wills, J., & Eriksson, O. (1998). Theoretical investigation of elastic properties of materials. *Journal of Applied Physics, 84*, 4891. https://doi.org/10.1063/1.368733